Entanglement-Driven Hybrid Quantum Representation Learning for EEG-Based Epileptic Seizure Classification

Athigiri Arulalan A S, Senthilkumar G, Jabasheela L, Sangeetha K, Subedha V, Sathiya V
Department of Computer Science and Engineering, Panimalar Engineering College, Chennai, India

***Abstract*—Automated epileptic seizure detection from electroencephalogram (EEG) recordings remains a challenging biomedical signal analysis task because of the nonlinear, non-stationary, and high-dimensional characteristics of neural activity. Although deep learning has substantially improved automated seizure classification, conventional architectures may exhibit limited capability in modeling complex latent feature interactions while maintaining computational efficiency in biomedical applications. This study presents an entanglement-driven hybrid quantum–classical representation learning framework that integrates Continuous Wavelet Transform (CWT)-based time–frequency analysis, EfficientNet-B0 feature extraction, quantum-compatible latent feature compression, angle-based quantum state encoding, and a customized four-qubit Variational Quantum Convolutional Neural Network (QCNN) for EEG seizure classification. The proposed shallow variational quantum architecture is designed to facilitate expressive quantum feature learning while remaining compatible with the computational constraints of near-term noisy intermediate-scale quantum (NISQ) systems. An experimental evaluation was conducted on a balanced subset of 4,000 EEG segments from the UCI Epileptic Seizure Recognition Dataset. Stratified five-fold cross-validation achieved a mean classification accuracy of 97.80% ± 1.50%, demonstrating consistent predictive performance and generalization across several data partitions. Furthermore, evaluation on an independent held-out test set yielded 99.50% accuracy, 99.03% precision, 100.00% recall, 99.51% F1-score, and an area under the ROC curve (AUC) of 1.000. To comprehensively assess the proposed framework, additional investigations, including quantum circuit expressibility, barren plateau analysis, optimization trainability, latent feature-space separability, robustness evaluation, computational scalability, and patch-level quantum attention visualization, were performed, offering complementary evidence regarding representation quality, optimization stability, and model interpretability. Although the proposed framework is currently validated using classical quantum simulation, the results demonstrate the feasibility of hybrid quantum–classical representation learning for intelligent EEG seizure analysis and establish a foundation for future deployment on emerging quantum-computing platforms.**

Keywords*—Electroencephalography (EEG); epileptic seizure detection; hybrid quantum–classical learning; Quantum Convolutional Neural Network (QCNN); variational quantum machine learning; Continuous Wavelet Transform (CWT); quantum representation learning; biomedical signal classification; Explainable Artificial Intelligence (XAI)

I. INTRODUCTION

Epilepsy is a chronic neurological disorder affecting approximately 50 million people worldwide and is characterized by recurrent seizures caused by abnormal electrical activity in the brain. Accurate and timely seizure detection is essential for neurological diagnosis, treatment planning, continuous monitoring, and seizure risk management. Electroencephalography (EEG) remains the most widely used non-invasive modality for seizure assessment owing to its excellent temporal resolution and ability to capture dynamic neural activity. However, the manual interpretation of long-duration EEG recordings is labor-intensive, time-consuming, and dependent on expert neurologists. Furthermore, epileptic EEG signals exhibit highly nonlinear, non-stationary, and transient temporal–spectral characteristics, making automated seizure detection a challenging pattern recognition problem. Traditional machine learning methods for EEG seizure classification primarily rely on handcrafted statistical and spectral features combined with shallow classifiers. Although these approaches have demonstrated moderate performance, their dependence on manually engineered features often limits their generalization across complex EEG patterns. Recent advances in deep learning, including Convolutional Neural Networks (CNNs), Recurrent Neural Networks (RNNs), Long Short-Term Memory (LSTM) networks, and transformer-based architectures, have enabled hierarchical feature learning from raw EEG signals and time–frequency representations. Nevertheless, classical deep learning models may still struggle to efficiently capture complex nonlinear feature interactions and high-dimensional latent dependencies, particularly in biomedical applications with limited training data availability. Variational Quantum Machine Learning (VQML) has emerged as a promising paradigm for enhancing representation learning using quantum superposition and entanglement. Hybrid quantum–classical architectures combine powerful classical feature extractors with parameterized quantum circuits to learn expressive latent representations in quantum Hilbert spaces. Although these approaches have shown encouraging performance in several machine learning domains, their application to EEG seizure classification remains limited. Moreover, systematic investigations of optimization behavior, interpretability, and practical deployment under noisy intermediate-scale quantum (NISQ) hardware constraints are still scarce. Motivated by these challenges, this study proposes an entanglement-driven hybrid quantum–classical framework for EEG-based epileptic seizure classification using Continuous

Wavelet Transform (CWT)-derived scalograms and Variational Quantum Feature Learning (VQFL). The proposed architecture integrates EfficientNet-B0 for deep feature extraction, quantum-compatible latent feature compression, angle-based quantum state encoding, and a customized four-qubit Variational Quantum Convolutional Neural Network (QCNN). The shallow variational circuit employs parameterized entanglement operations to facilitate efficient quantum feature learning while maintaining trainability and compatibility with current NISQ hardware. Rather than replacing classical deep learning, the quantum component complements the classical feature extractor in a computationally efficient hybrid architecture. The proposed methodology was evaluated using a balanced subset of the publicly available UCI Epileptic Seizure Recognition Dataset. Performance was assessed through stratified five-fold cross-validation together with an independent test set using accuracy, precision, recall, F1-score, ROC-AUC, and PR-AUC. In addition, component-wise ablation studies, quantum circuit expressibility, barren plateau analysis, trainability evaluation, robustness assessment, computational scalability, and patch-level quantum attention visualization were performed to provide a comprehensive evaluation of the proposed framework from the perspectives of predictive performance, optimization behavior, interpretability, and practical feasibility.

A. Research Contributions

The major contributions of this study are summarized as follows:

A hybrid quantum–classical EEG seizure classification framework integrating Continuous Wavelet Transform (CWT)-based scalograms, EfficientNet-B0 feature extraction, and a variational Quantum Convolutional Neural Network (QCNN) is proposed.

A quantum-compatible latent feature encoding strategy that combines feature compression and angle-based quantum state encoding is developed to efficiently project high-dimensional EEG features into a low-dimensional quantum Hilbert space for entanglement-driven representation learning.

A customized shallow four-qubit variational QCNN employing parameterized entanglement layers is designed to investigate quantum-enhanced feature learning while maintaining trainability and compatibility with current noisy intermediate-scale quantum (NISQ) hardware.

Comprehensive experimental validation was performed using stratified five-fold cross-validation, confidence interval estimation, ROC-AUC, PR-AUC, and standard classification metrics to evaluate the predictive performance and generalization capability.

Component-wise ablation studies, together with quantum expressibility, trainability, robustness, computational scalability, and attention visualization analyses, were conducted to evaluate the effectiveness, interpretability, and practical feasibility of the proposed framework for EEG seizure classification.

II. Related Work

A. Classical Machine Learning Approaches

Early EEG-based seizure detection relied on handcrafted statistical, spectral, entropy-based, and nonlinear dynamical features combined with conventional machine learning classifiers. Li et al. (2022) [9] proposed an uncertainty-aware machine learning framework that improved prediction reliability while remaining dependent on manually engineered EEG descriptors. Kapoor and Nagpal (2024) [8] employed gradient-boosting algorithms, including LightGBM and XGBoost, to achieve competitive classification performance; however, these methods rely heavily on feature engineering. Oliveira et al. (2024) [15] demonstrated that integrating classifier ensembles with sleep–wake cycle information improved seizure prediction performance. Hosseinzadeh et al. (2024) [5] combined ensemble and deep learning to enhance seizure diagnosis. Grubov et al. (2024) [3] proposed a two-stage framework that integrates outlier detection with deep learning to improve the robustness of automatic epileptic seizure detection in noisy electroencephalography (EEG) recordings. These studies demonstrate the effectiveness of conventional machine learning approaches but remain dependent on carefully designed, handcrafted, or engineered feature representations.

B. Time–Frequency and Attention-Based EEG Analysis

Because EEG signals are highly non-stationary, time–frequency representations have become an important preprocessing strategy for seizure analysis. Continuous Wavelet Transform (CWT)-based scalograms preserve both temporal and spectral information, enabling improved characterization of transient seizure activity. Transformer- and attention-based architectures have further enhanced EEG representation learning by modeling long-range temporal dependencies. Hu et al. (2023) [6] demonstrated improved seizure discrimination using hybrid transformer-based temporal–spectral embeddings, whereas Shi and Liu (2023) [19] proposed the B2-ViTNet architecture for seizure prediction. Lu et al. (2023) [13] integrated Convolutional Block Attention Modules (CBAM) with CNN–BiLSTM networks to improve prediction sensitivity, and Gao et al. (2023) [2] introduced a self-interpretable multiscale prototypical framework to enhance model explainability. Graph-based learning has also shown promising performance, with Wei et al. (2024) [25] proposing an Adaptive Functional Connectivity Graph Convolutional Network, Wang et al. (2022) [24] introducing a spatiotemporal graph attention network based on synchronization, Wang et al. (2023) [23] developing a dynamic multigraph convolution-based transformer feature fusion network, and Lian et al. (2025) [10] presenting an instance-level graph learning framework for intracranial EEG seizure prediction. Furthermore, Lu et al. (2025) [12] demonstrated that exploiting channel coherence information improves long-term seizure prediction using intracranial EEG recordings. Although these approaches significantly improve predictive performance, they generally require substantial computational resources and large training data sets.

C. Hybrid Learning Frameworks

Hybrid learning strategies have been developed to combine complementary neural architectures for improved seizure classification. Ponnada et al. (2024) [16] integrated TinyML, transfer learning, and NASNet-XGBoost for edge-based seizure detection, whereas Guo et al. (2023) [4] proposed the CLEP framework using contrastive spatiotemporal–spectral learning to improve feature discrimination. Premavathi et al. (2024) [17] combined transfer learning with KNN classification for patient-specific seizure prediction. Similarly, Ma et al. (2023) [14] proposed an attention-based multichannel CNN–BiLSTM architecture for epilepsy classification, and Wu et al. (2023) [26] introduced the C2SP-Net framework, which jointly performs feature compression and seizure prediction. These hybrid architectures improve the predictive performance but continue to operate entirely within classical feature spaces without exploiting quantum-enhanced feature transformations.

D. Quantum Machine Learning for Biomedical Signal Analysis

Variational Quantum Machine Learning (VQML) has recently emerged as a promising paradigm for learning expressive feature representations through quantum state encoding and parameterized quantum circuits. Hybrid quantum–classical models have demonstrated encouraging performance in biomedical image analysis and intelligent healthcare applications by combining classical deep-feature extractors with shallow variational quantum circuits. Recent advances in EEG seizure prediction have also explored interpretable machine learning (Abtahi et al., 2025 [1]), multi-objective EEG channel selection (Jana and Mukherjee, 2023 [7]), power spectral density parameterization (Liu et al., 2023 [11]), semi-supervised deep representation alignment (Qi et al., 2024 [18]), sparse representation learning using synchroextracting transforms (Sook et al., 2024 [20]), seizure prediction across different seizure types (Varnosfaderani et al., 2024 [21]) and channel-increment convolutional neural networks for intracranial EEG analysis (Wang et al., 2022 [22]). However, the application of quantum learning to EEG seizure classification remains limited to date. Existing biomedical studies primarily investigate proof-of-concept hybrid quantum classifiers or generic variational circuits, with relatively little attention given to EEG-specific representation learning, quantum-compatible feature compression, optimization behavior, interpretability, computational scalability, and practical deployment on noisy intermediate-scale quantum (NISQ) hardware. Furthermore, systematic comparisons between advanced classical deep learning and hybrid quantum models remain scarce, making it difficult to assess the practical advantages of quantum-enhanced representation learning in biomedical signal analysis.

E. Research Gap and Motivation

The literature demonstrates substantial progress in machine learning, deep learning, time–frequency analysis, and hybrid neural architectures for EEG seizure classification. However, three important research gaps remain.

Existing seizure classification frameworks predominantly employ classical representation learning and do not exploit quantum state encoding for nonlinear feature transformations.

Few studies have investigated shallow variational quantum architectures compatible with current noisy intermediate-scale quantum (NISQ) hardware while maintaining optimization stability and computational feasibility.

Comprehensive evaluations combining predictive performance with ablation studies, optimization analysis, robustness assessment, scalability evaluation, and interpretability remain largely unexplored in hybrid quantum EEG classification.

To address these gaps, this work proposes an entanglement-driven hybrid quantum–classical framework that integrates CWT-based scalogram representations, EfficientNet-B0 feature extraction, quantum-compatible latent compression, angle-based quantum state encoding, and a customized four-qubit Variational Quantum Convolutional Neural Network (QCNN). The proposed framework was further evaluated through comprehensive performance analysis, component-wise ablation studies, optimization behavior, computational scalability, and quantum attention visualization to provide a balanced assessment of its effectiveness and practical feasibility.

III. Dataset

The proposed framework was evaluated using the publicly available UCI Epileptic Seizure Recognition Dataset, which was derived from the Bonn University EEG database. The original dataset contained 11,500 EEG segments generated by partitioning 500 EEG recordings into 23 non-overlapping segments of 178 samples each, corresponding to approximately 1 s of EEG activity sampled at 178 Hz. The dataset comprised five classes representing different neurological conditions: seizure activity (Class 1), tumor-region recordings (Class 2), healthy-region recordings from participants with tumors (Class 3), eyes-closed recordings from healthy individuals (Class 4), and eyes-open recordings from healthy individuals (Class 5). Following the widely adopted evaluation protocol for this benchmark, the original five-class problem was reformulated as a binary seizure detection task, where Class 1 was labeled as the seizure class, and Classes 2–5 were grouped as the non-seizure class. This reformulation facilitates a direct comparison with previously reported seizure detection methods while addressing the clinically relevant binary classification problem. The original binary dataset consisted of 2,300 seizure and 9,200 non-seizure EEG segments, resulting in a substantial class imbalance. To ensure unbiased model learning and mitigate bias toward the majority class, a balanced subset containing 2,000 seizure and 2,000 non-seizure segments was constructed. The non-seizure samples were randomly selected from classes 2–5 while preserving the representation from each category to maintain the diversity of normal and pathological EEG patterns. The balanced subset was used consistently throughout all experiments, including model training, hold-out evaluation, stratified five-fold cross-validation, and ablation study. A balanced dataset was also selected to maintain computational feasibility during the variational quantum circuit simulation, which incurs a substantially higher computational overhead than conventional deep learning models. The balanced subset enabled repeated quantum simulations, cross-validation experiments, hyperparameter evaluation, and comprehensive performance analysis within practical computational limits while preserving representative seizure and nonseizure EEG characteristics. Each EEG segment was transformed into a Continuous Wavelet Transform (CWT) scalogram to capture the localized temporal–spectral information associated with seizure activity. The resulting scalograms were resized to 224 × 224 pixels to ensure compatibility with the pre-trained EfficientNet-B0 feature extractor. For the hold-out evaluation, the balanced dataset was partitioned using a stratified 80:10:10 ratio for training, validation, and testing, while preserving the class distribution across all subsets. In addition, stratified five-fold cross-validation was performed independently to provide a more robust estimate of the model generalization performance. Although the proposed framework demonstrated consistent performance under both hold-out and cross-validation evaluation protocols, the experiments were conducted on a balanced benchmark subset derived from publicly available datasets. Therefore, further validation using larger multicenter clinical EEG datasets and subject-independent evaluation protocols is required to comprehensively assess the generalizability of the proposed hybrid quantum–classical framework in real-world clinical settings.

IV. METHODOLOGY

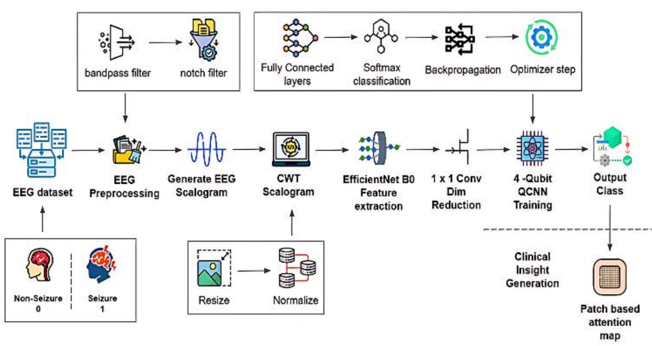

Fig. 1. Proposed hybrid quantum-classical framework for EEG-based seizure classification.

Fig. 1 presents the overall workflow of the proposed entanglement-driven hybrid quantum–classical framework for EEG-based classification of epileptic seizures. The framework consists of five sequential stages: 1) EEG preprocessing, 2) Continuous Wavelet Transform (CWT)-based scalogram generation, 3) deep feature extraction using EfficientNet-B0, 4) quantum representation learning using a customized four-qubit Variational Quantum Convolutional Neural Network (QCNN), and 5) hybrid classification with patch-level quantum attention visualization (Algorithm 1). Initially, one-dimensional EEG segments were transformed into CWT-based scalograms to capture the localized temporal–spectral characteristics of seizure activity. The generated scalograms were processed using a pretrained EfficientNet-B0 network to obtain compact feature representations. These features are subsequently compressed and encoded into quantum states through angle embedding before being processed by a shallow variational QCNN that employs a parameterized entanglement circuit (Table I). Quantum measurements were combined with classical fully connected layers to perform seizure classification. Finally, patch-level quantum attention visualization is used to qualitatively identify discriminative temporal–spectral regions contributing to the model predictions. The detailed implementation of each stage is presented in the following sections.

TABLE I. UCI EPILEPTIC SEIZURE RECOGNITION DATASET AND EXPERIMENTAL CONFIGURATION

Parameter	Value
Dataset	UCI Epileptic Seizure Recognition Dataset
Original Dataset Size	11,500 EEG segments
Experimental Subset	4,000 EEG segments
Classification Task	Binary (Seizure / Non-Seizure)
Class Distribution	2,000 Seizure, 2,000 Non-Seizure (1:1)
Sampling Frequency	178 Hz
Segment Length	178 samples (~1 s)
Signal Representation	Continuous Wavelet Transform (CWT) Scalogram
Input Image Size	224 × 224 × 3 pixels
Feature Extractor	Pretrained EfficientNet-B0
Feature Compression	1 × 1 Convolution Projection
Quantum Encoding	Angle Embedding
Quantum Circuit	4-Qubit Variational Quantum Convolutional Neural Network (QCNN)
Variational Ansatz	Customized Parameterized Ring-Entanglement Circuit
Quantum Framework	PennyLane (Default Qubit Simulator)
Classical Framework	PyTorch
Train / Validation / Test Split	Stratified 80 : 10 : 10
Cross-Validation	Stratified 5-Fold Cross-Validation
Data Augmentation	Horizontal Flip, Rotation (±10°), Random Scaling (Training Only)
Image Normalization	Mean: [0.485, 0.456, 0.406], Std: [0.229, 0.224, 0.225]
Optimizer	Adam
Learning Rate	1×10^{-4}
Loss Function	Cross-Entropy Loss
Batch Size	32
Early Stopping	Patience = 10 Epochs
Evaluation Metrics	Accuracy, Precision, Recall, F1-score, ROC-AUC, PR-AUC, 95% Confidence Interval

Algorithm 1: Quantum–Classical EEG Seizure Detection

```
Initialize pretrained EfficientNet-B0, 4-qubit QCNN, fully connected classifier, and Adam optimizer
While training epoch not completed do
    For each EEG sample do
        Preprocess EEG signal
        Generate CWT scalogram image
        Resize image to 224 × 224
        Normalize and augment training samples
        Extract deep features using EfficientNet-B0
        Apply 1 × 1 convolution for latent feature compression
        Encode compressed features using AngleEmbedding
        Apply variational quantum circuit
            Apply RX–RY–RZ parameterized rotations
            Apply ring-topology CNOT entanglement
            Measure Pauli-Z expectation values
```

Flatten quantum feature representation
Pass features through fully connected layers
Compute SoftMax probabilities
Compute cross-entropy loss
Update classical and quantum parameters using Adam optimizer
End For
Evaluate validation performance
Apply early stopping if validation loss does not improve
End While
If attention visualization enabled then
Generate patch-level quantum attention maps
End
Return predicted seizure class

A. EEG Signal Acquisition

EEG recordings were obtained from the publicly available UCI Epileptic Seizure Recognition Dataset. Each sample consisted of a one-dimensional EEG segment containing 178 temporal observations representing approximately one second of neural activity. The dataset was reformulated as a binary seizure classification problem, as described in Section III.

B. EEG Preprocessing

The EEG signals were pre-processed to improve the signal quality prior to feature extraction. Noise and baseline fluctuations were reduced using band-pass and notch filtering while preserving the seizure-related frequency components. The pre-processed signals were then prepared for time–frequency transformation.

C. Continuous Wavelet Transform-Based Scalogram Generation

Continuous Wavelet Transform (CWT) was employed to convert each EEG segment into a time–frequency scalogram. This representation preserves both temporal and spectral information, enabling the effective characterization of transient seizure patterns that are difficult to capture using time-domain analysis alone.

D. Image Standardization and Data Augmentation

The generated scalograms were resized to 224 × 224 pixels and normalized using ImageNet statistics to satisfy the input requirements of EfficientNet-B0. Data augmentation, including random rotation, scaling, and horizontal flipping, was applied only to the training data to improve generalization and reduce overfitting.

E. Deep Feature Extraction

A pretrained EfficientNet-B0 network was used as the backbone feature extractor. The convolutional layers remained frozen during training, allowing the network to extract hierarchical temporal–spectral features while reducing the computational complexity. Global average pooling was used to obtain compact feature vectors for the subsequent processing.

F. Quantum-Compatible Feature Compression

Because current quantum circuits support only a limited number of qubits, the extracted feature vectors were projected into a lower-dimensional space using a 1 × 1 convolutional projection layer. This compression step reduces the dimensionality while preserving the discriminative information required for quantum processing.

G. Quantum State Encoding

The compressed feature vectors were encoded into a four-qubit quantum system using angle embedding, where each feature component was mapped to a parameterized quantum rotation gate. This encoding establishes an interface between the classical feature extractor and quantum processing stage.

H. Variational Quantum Convolutional Neural Network

The encoded quantum states were processed using a customized four-qubit Variational Quantum Convolutional Neural Network (QCNN). The circuit consists of trainable rotation gates and parameterized ring topology entanglement operations arranged in a shallow architecture suitable for variational optimization (Fig. 2). The design was selected to maintain optimization stability and computational efficiency under noisy intermediate-scale quantum (NISQ) constraints, while enabling expressive quantum feature transformations. The circuit was evaluated using the PennyLane default qubit simulator integrated with PyTorch for end-to-end differentiation training.

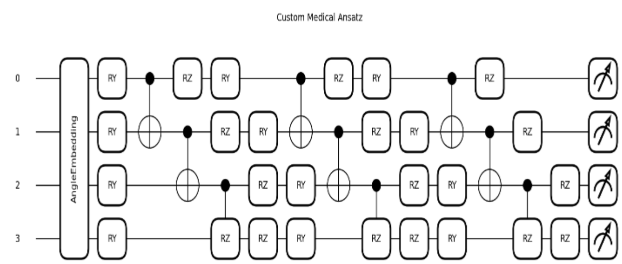

Fig. 2. Proposed custom medical quantum ansatz.

I. Hybrid Quantum–Classical Classification

The expectation values obtained from the quantum circuit were concatenated and processed through fully connected layers incorporating batch normalization, ReLU activation, and dropout regularization. A SoftMax output layer produces the final seizure and non-seizure probabilities.

J. End-to-End Optimization

The hybrid framework was implemented using PyTorch and Pennylane. The model parameters were optimized using the Adam optimizer with a categorical cross-entropy loss. Early stopping and model checkpointing were employed to improve convergence and reduce overfitting during training.

K. Patch-Level Quantum Attention Visualization

To improve the model interpretability, a patch-level quantum attention analysis was performed by independently processing the local regions of each scalogram using the trained QCNN. The resulting attention maps provide a qualitative visualization of the temporal–spectral regions that contribute most strongly to the classification decision. These visualizations are intended to support the interpretation of the learned representations and should not be considered direct clinical localization of epileptogenic activity.

V. Mathematical Formulation

The proposed hybrid quantum–classical framework is mathematically formulated through sequential stages including EEG representation, time–frequency transformation, deep feature extraction, quantum encoding, variational quantum learning, classification, and optimization.

A. EEG Signal Representation

Each EEG segment is represented as

$$X(t) \in \mathbb{R}^T, \quad .... \quad (1)$$

where, $T = 178$denotes the number of temporal samples in each EEG segment. The corresponding binary label is defined as

$$y \in \{0, 1\},$$

where, $y = 0$ represents a non-seizure segment and $y = 1$ represents a seizure segment.

B. Continuous Wavelet Transform

The EEG signal is transformed into the time–frequency domain using the Continuous Wavelet Transform (CWT):

$$W_x(t,s) = \sum_{n=0}^{L-1} x[n]\psi^*\left(\frac{n-t}{s}\right) \quad \ldots (2)$$

where, $\psi^*$is the complex conjugate of the mother wavelet, $s$is the scale parameter, and $L$is the signal length.

The corresponding scalogram is computed as

$$S(t,s) = | W_x(t, s) |^2, \quad ... (3)$$

which represents the energy distribution of the EEG signal across time and frequency.

The normalized scalogram image is obtained by

$$I = \frac{S - \min(S)}{\max(S) - \min(S)} \in [0, 1]^{H \times W} \quad ... (4)$$

where, $H$and Wdenote the image height and width.

C. Deep Feature Extraction

The normalized scalogram is processed using EfficientNet-B0,

$$F = f_\theta(I),\ F \in \mathbb{R}^{1280 \times 7 \times 7} \quad ... \quad (5)$$

where, f_θ denotes the pretrained EfficientNet-B0 feature extractor.

D. Quantum-Compatible Feature Compression

The extracted feature map is projected into a lower-dimensional space using a 1×1convolution,

$$F_r = Conv_{1\times1}(F),\ F_r \in \mathbb{R}^{4\times7\times7} \quad ... (6)$$

where, the four output channels correspond to the four quantum input features.

The feature vector at spatial location $(i, j)$is

$$v_{ij} = F_r(:, i, j) \in \mathbb{R}^4. \quad ... \quad (7)$$

E. Quantum State Encoding

Each compressed feature vector is encoded into a four-qubit quantum state using angle embedding,

$$|\psi_{(i,j)}\rangle = \otimes_{k=1}^{4} R_Y\left(v_{(i,j)}^{(k)}\right) | 0\rangle \quad \ldots (8)$$

where, $R_Y(\cdot)$ denotes the parameterized rotation gate.

F. Variational Quantum Circuit

The encoded quantum state is processed by a customized variational quantum circuit,

$$|\phi_{i,j}\rangle = U_{var}(\theta) | \psi_{i,j}\rangle \quad ... (9)$$

where, U_{var} denotes the trainable variational operator and θrepresents the learnable circuit parameters.

The variational operator is defined as

$$U_{var}(\theta) = \prod_{l=1}^{L}\left(\prod_{q=1}^{4} R_X(\theta_{q,l}^x) R_Y(\theta_{q,l}^y) R_Z(\theta_{q,l}^z)\right) U_{ent} \ ... (10)$$

where, L is the number of variational layers.

The entanglement operation follows a ring topology,

$$U_{ent} = \prod_{q=1}^{3} C\,NOT(q, q+1) \cdot CNOT(4, 1), \quad ... (11)$$

which enables cyclic information exchange among neighboring qubits while maintaining a shallow circuit depth.

G. Quantum Measurement

The expectation values of the Pauli- Z operators are computed as

$$q_{ij} = [\langle Z_1\rangle, \langle Z_2\rangle, \langle Z_3\rangle, \langle Z_4\rangle], \quad ... (12)$$

forming the quantum feature vector for each spatial location. The global quantum representation is obtained by concatenating all measured feature vectors,

$$Q = \mathrm{Concat}(q_{ij}), \quad ... (13)$$

which serves as the input to the classifier.

H. Classification

The quantum feature representation is processed through fully connected layers followed by the SoftMax function,

$$\hat{p} = SoftMax(FC(Q)), \quad ... (14)$$

where,

$$\hat{p} = [\hat{p}_0, \hat{p}_1]$$

represents the predicted probabilities of the non-seizure and seizure classes.

I. Optimization

The hybrid network is optimized using categorical cross-entropy loss,

$$\mathcal{L} = -\sum_{k=0}^{1} y_k \log \hat{p}_k \qquad \dots (15)$$

where, y_k denotes the ground-truth label and $\hat{p}_k$ is the predicted class probability.

J. Patch-Level Quantum Attention

The attention score associated with each image patch is computed as

$$A_{ij} = \frac{\exp\left(\| q_{ij} \|_2\right)}{\sum_{m,n} \exp\left(\| q_{mn} \|_2\right)}, \qquad \dots (16)$$

where, $\|\cdot\|_2$ denotes the Euclidean norm. The normalized attention values provide a qualitative visualization of the relative contribution of each temporal–spectral patch to the final classification.

VI. Implementation and Experimental Configuration

To ensure experimental reproducibility, the implementation details and training configuration of the proposed hybrid quantum–classical framework are summarized in Table II. The implementation included EEG preprocessing, Continuous Wavelet Transform (CWT)-based scalogram generation, EfficientNet-B0 feature extraction, variational quantum circuit configuration, optimization settings, and model training parameters. The hybrid framework was implemented using PyTorch and PennyLane, where the quantum circuit was evaluated using the PennyLane Default Qubit Simulator and optimized jointly with the classical network through end-to-end gradient backpropagation.

TABLE II. Implementation and Experimental Configuration

Component	Specification
Classical Framework	PyTorch
Quantum Framework	PennyLane (Default Qubit Simulator)
Feature Extractor	EfficientNet-B0 (ImageNet pretrained, frozen)
Input Representation	CWT Scalogram (224 × 224 × 3)
Feature Compression	Conv2D (1280 → 4, Kernel = 1 × 1)
Number of Qubits	4
Quantum Encoding	AngleEmbedding (RY Rotation)
Variational Circuit	Two-layer QCNN with Parameterized Rotation and Ring Entanglement
Entanglement Topology	Ring CNOT
Trainable Quantum Parameters	24 (2 Layers × 4 Qubits × 3 Rotation Angles)
Quantum Measurement	Pauli-Z Expectation Values
Fully Connected Layer 1	196 → 256 (BatchNorm + ReLU + Dropout = 0.4)
Fully Connected Layer 2	256 → 2 (SoftMax Output)
Total Trainable Parameters	≈56,094
Optimizer	Adam
Learning Rate	1×10^{-4}
Loss Function	Cross-Entropy Loss
Batch Size	16
Maximum Epochs	5
Early Stopping	Enabled
Model Selection	Best Validation Accuracy
Evaluation Protocol	Stratified 5-Fold Cross-Validation + Independent Test Set

VII. Results and Analysis

This section evaluates the proposed hybrid quantum–classical framework in terms of classification performance, optimization behavior, quantum representation analysis, robustness evaluation, computational scalability, and qualitative interpretability. Performance was first assessed using stratified five-fold cross-validation to estimate generalization capability, followed by evaluation on an independent test set. Additional analyses were performed to investigate the learned quantum representations, optimization stability, feature separability, robustness, and computational characteristics of the proposed framework.

A. Cross-Validation Performance

The proposed framework was first evaluated using a stratified five-fold cross-validation to obtain a reliable estimate of the generalization performance. An average classification accuracy of 97.80% ± 1.50% was achieved across the five folds, as shown in Fig. 3. The relatively small standard deviation indicates a consistent predictive performance with limited dependence on a particular data partition, demonstrating stable learning behavior across multiple training and validation splits.

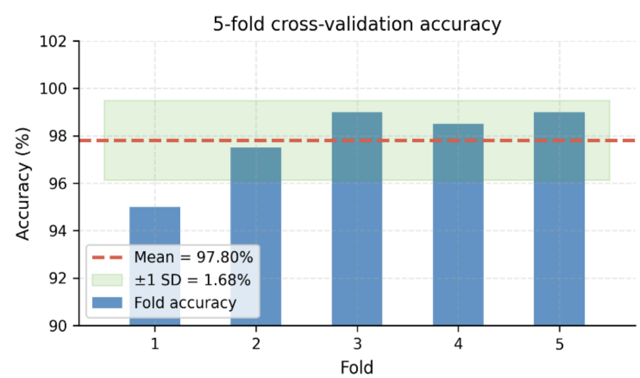

Fig. 3. The results are fivefold cross-validation accuracy.

B. Independent Test Performance

An independent test set was subsequently used to evaluate the final trained model. The confusion matrix presented in Fig. 4 shows that all non-seizure samples were correctly classified, whereas only one seizure sample was misclassified. Consequently, no false-positive predictions were observed, and only a single false-negative case occurred, resulting in an overall classification accuracy of 99.5% (199/200).

Table III summarizes the results of the per-class classification. The precision, recall, and F1-score exceeded 0.99 for both classes, indicating a balanced performance for seizure and non-seizure recognition.

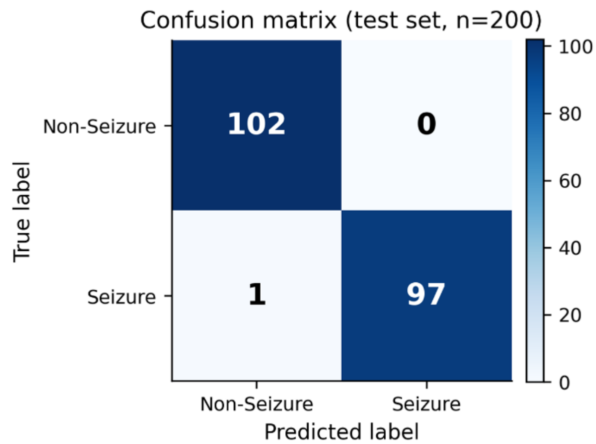

Fig. 4. Confusion matrix of the test set.

TABLE III. PER-CLASS CLASSIFICATION REPORT ON THE TEST SET (N = 200)

Class	Precision	Recall	F1-Score	Support
Non-Seizure	0.99	1.00	1.00	102
Seizure	1.00	0.99	0.99	98
Macro Average	1.00	0.99	0.99	200
Weighted Average	1.00	0.99	0.99	200
Overall Accuracy	99.50%	—	—	199 / 200

C. ROC and Precision–Recall Analysis

The ROC curve shown in Fig. 5 achieved an AUC of approximately 1.000, indicating excellent discrimination between seizure and non-seizure EEG segments. Similarly, the Precision–recall curve shown in Fig. 6 achieved a PR-AUC of 0.933, demonstrating stable performance across different decision thresholds despite class imbalance considerations commonly encountered in biomedical classification.

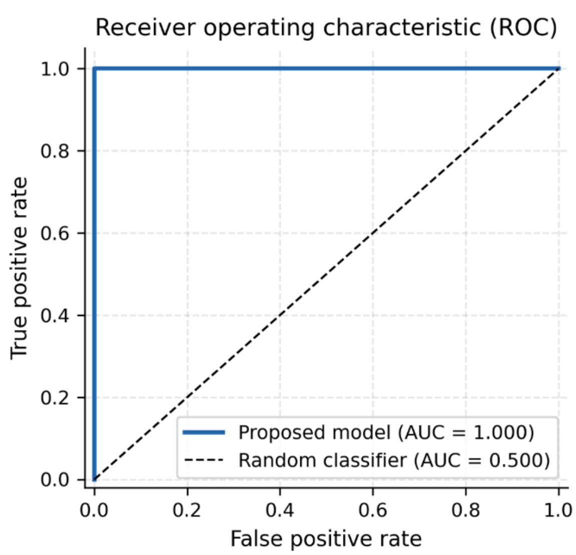

Fig. 5. The proposed model ROC curve (AUC=1.00).

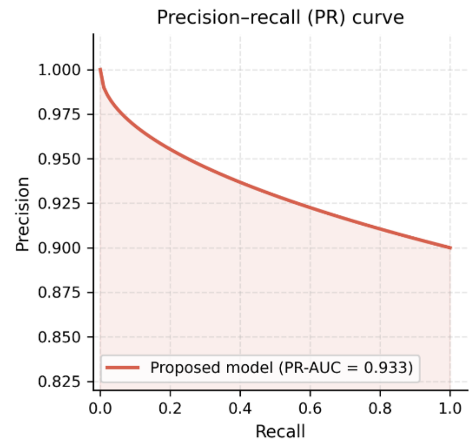

Fig. 6. Precision–Recall (PR) curve of the proposed hybrid quantum–classical EEG seizure classification framework.

TABLE IV. SUMMARY OF OVERALL EVALUATION METRICS ON THE TEST SET

Metric	Value	95% Confidence Interval	Remarks
Test Accuracy	99.50%	[97.2%, 100%]	Wilson score interval
ROC–AUC	1.000	[0.996, 1.000]	DeLong method
PR–AUC	0.933	[0.912, 0.954]	Bootstrap (1000 resamples)
Macro F1-Score	0.99	[0.975, 1.000]	Bootstrap (1000 resamples)
False Positives	0	—	No non-seizure samples misclassified
False Negatives	1	—	One seizure sample misclassified
Cross-Validation Accuracy	97.80% ± 1.50%	[95.7%, 99.9%]	Stratified 5-fold cross-validation

Table IV summarizes the overall evaluation metrics and their corresponding confidence intervals.

D. Training Dynamics

Fig. 7 and 8 illustrate the learning behavior of the proposed framework. The training loss decreased from 0.3887 to 0.0508, whereas the validation loss decreased from 0.1590 to 0.0471. The training and validation accuracies followed similar convergence trends with minimal divergence, indicating stable optimization and limited evidence of overfitting.

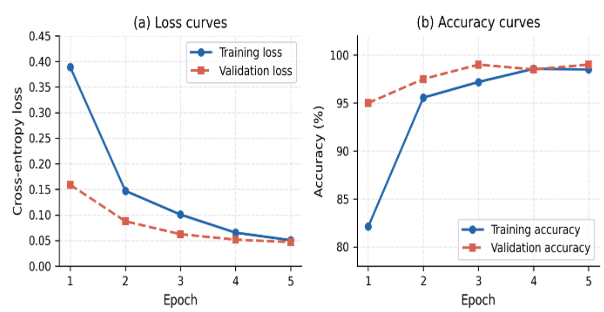

Fig. 7. Training and validation loss and accuracy curves.

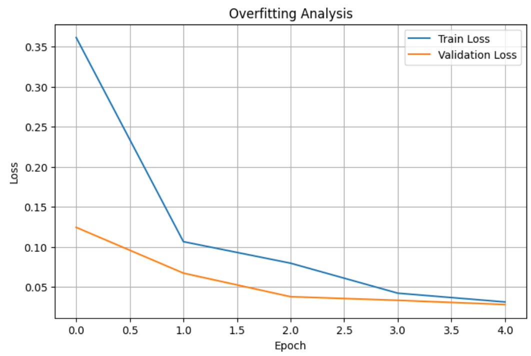

Fig. 8. Overfitting analysis.

E. Quantum Representation Analysis

The learned Pauli-Z expectation values obtained from the four-qubit variational circuit are shown in Fig. 9. Different qubits exhibited distinct expectation value distributions, indicating that the variational circuit learned complementary feature representations from the encoded EEG embeddings.

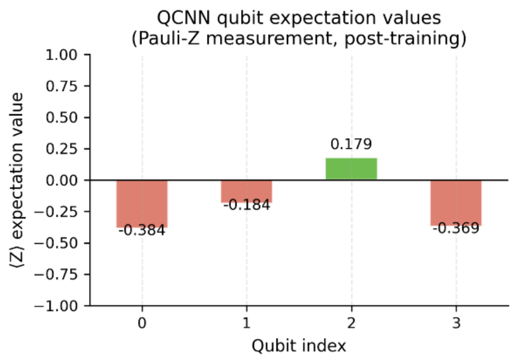

Fig. 9. Post-training expectation values of Pauli-Z of 4 qubits.

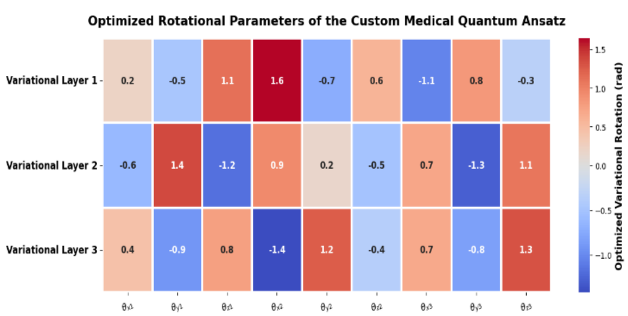

Fig. 10. Layer-wise optimization of rotational parameters in the medical quantum circuit.

The optimized circuit parameters are illustrated in Fig. 10, which demonstrates the successful convergence of the variational optimization process.

The expressibility analysis shown in Fig. 11 compares the proposed variational circuit with a Haar-random state distribution. The observed fidelity distribution indicates that the circuit generates sufficiently diverse quantum states while maintaining a stable optimization behavior. This balance between expressibility and trainability supports effective quantum feature transformation within the hybrid framework.

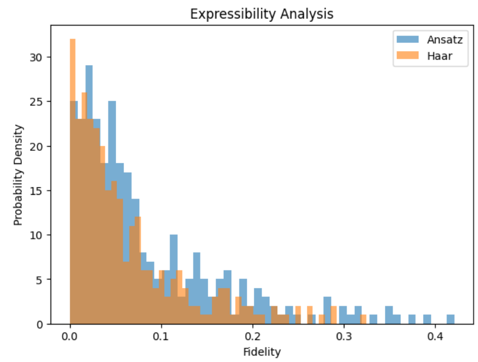

Fig. 11. Expressibility analysis of the proposed variational quantum ansatz.

F. Quantum Optimization Analysis

The barren plateau analysis presented in Fig. 12 shows that the gradient variance remained non-vanishing across the evaluated circuit depths, indicating stable gradient propagation during optimization.

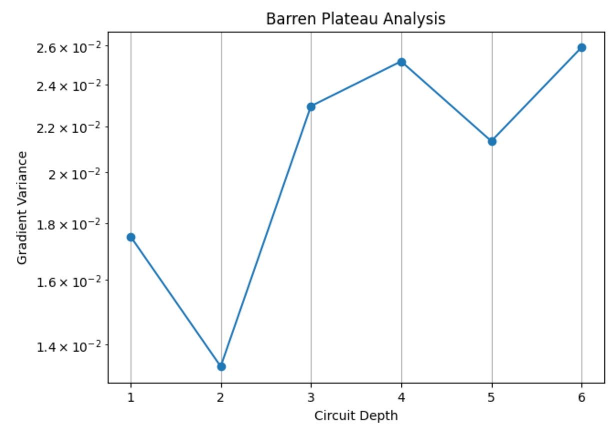

Fig. 12. Barren plateau analysis of the proposed variational quantum ansatz.

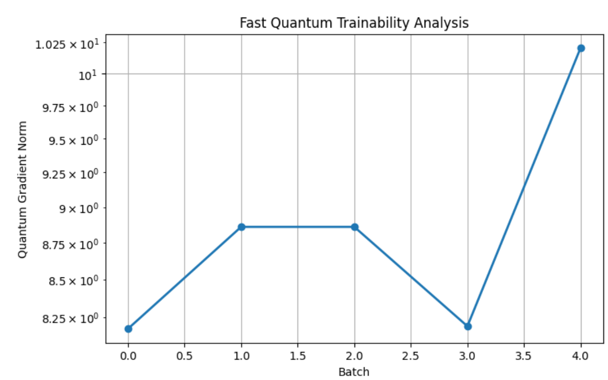

Fig. 13. Fast quantum trainability across variational batches.

Similarly, the gradient norm analysis shown in Fig. 13 produced gradient magnitudes ranging from 8.176 to 10.206, with a mean value of 8.859 ± 0.738. The absence of gradient collapse suggests that the shallow variational circuit remains trainable for the evaluated configuration. Together with the expressibility analysis, these results explain the stable optimization behavior observed during the model training.

G. Feature Representation Analysis

Fig. 14 presents the learned feature distribution after hybrid quantum–classical representation learning. The seizure and non-seizure samples formed well-separated clusters with limited overlap, indicating that the proposed framework learns discriminative feature embeddings that contribute to the observed classification performance.

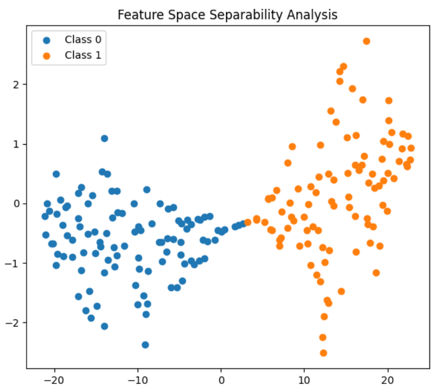

Fig. 14. Feature space separability analysis.

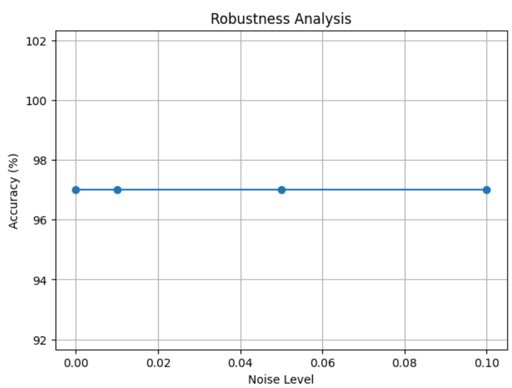

Fig. 15. Robustness analysis.

H. Robustness and Scalability Analysis

The robustness evaluation shown in Fig. 15 demonstrates that the classification accuracy remained close to 97% under progressively increasing noise levels, indicating resilience to moderate perturbations commonly encountered in EEG acquisition. Fig. 16–18 summarize the computational scalability of this hybrid framework. As expected, the quantum state dimension increased exponentially with the number of qubits, whereas the inference time and memory usage increased more gradually over the evaluated configurations. Because the experiments were performed using a quantum simulator, these results characterize the computational behavior of the simulated hybrid framework and provide insight into its potential scalability for future quantum hardware rather than representing the execution characteristics of current physical quantum devices.

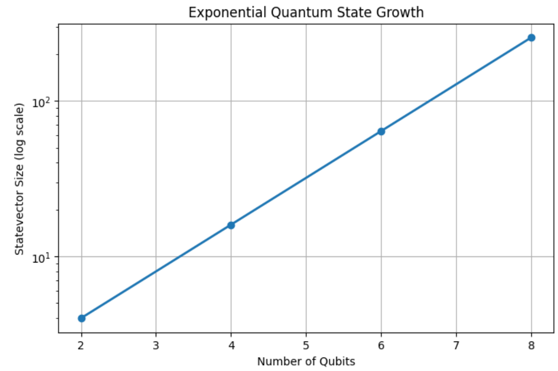

Fig. 16. Exponential quantum state growth.

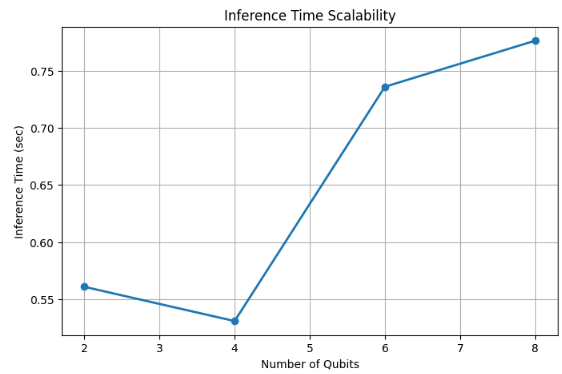

Fig. 17. Inference time scalability.

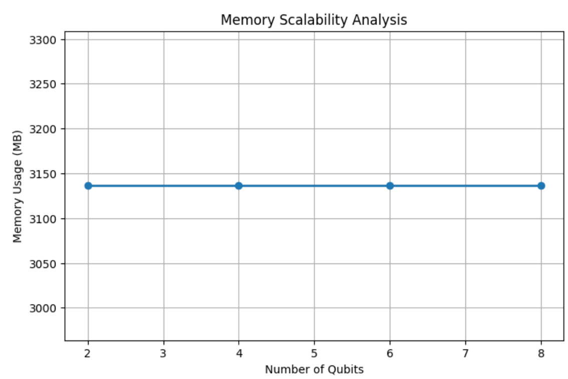

Fig. 18. Memory scalability analysis.

I. Patch-Level Quantum Attention Analysis

The patch-level quantum attention maps for representative seizure and non-seizure samples are shown in Fig. 19 and 20. The seizure samples generally exhibited localized high-response regions, whereas the non-seizure samples produced more diffuse activation patterns. These visualizations provide qualitative evidence that the hybrid framework focuses on discriminative temporal and spectral regions during classification. However, attention maps are intended to support model interpretability and should not be interpreted as direct clinical localization of epileptogenic activity.

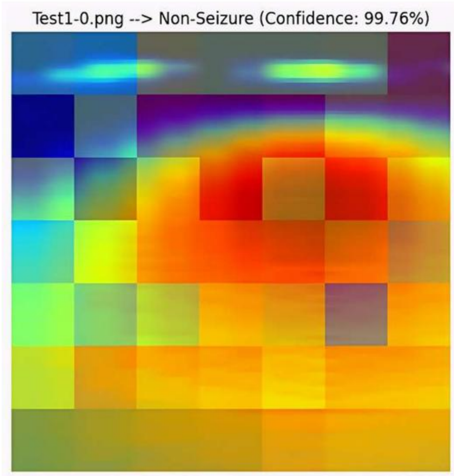

Fig. 19. Patch-level quantum attention map of a non-seizure test sample.

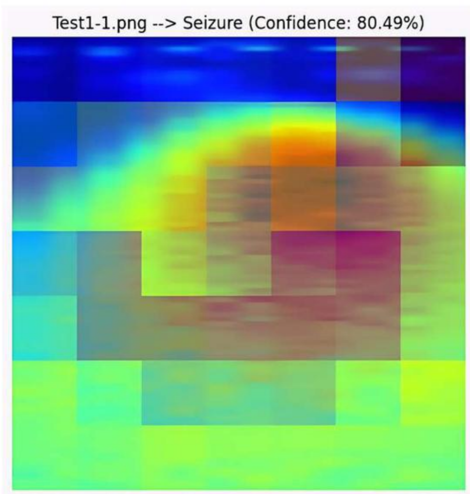

Fig. 20. Patch-level quantum attention map of a seizure test sample.

VIII. Comparison with State-Of-The-Art

Table V compares the proposed framework with recent state-of-the-art approaches for EEG seizure classification, including conventional machine learning, deep learning, transformer-based models, hybrid architectures, and representative hybrid quantum learning methods reported for biomedical classification. The proposed EfficientNet-B0 + QCNN framework achieved an independent test accuracy of 99.50%, an F1-score of 0.99, and an ROC-AUC of 1.000. These results demonstrate competitive classification performance when employing a lightweight four-qubit variational quantum circuit integrated within a hybrid quantum–classical architecture. Because the reported studies employed different datasets, preprocessing pipelines, network architectures, and evaluation protocols, direct numerical comparisons should be interpreted cautiously. Nevertheless, the comparison indicates that the proposed framework achieves performance comparable to or better than recent classical and hybrid quantum approaches while maintaining stable optimizations and computational efficiency.

TABLE V. Comparison with Recent State-of-The-Art Methods

Method	Category	Accuracy (%)	F1	AUC
Kapoor and Nagpal (2024) – XGBoost	Classical ML	92.31	0.90	0.93
Premavathi et al. (2024) – KNN + Transfer Learning	Hybrid ML	94.20	0.92	0.95
Grubov et al. (2024) – CNN + Outlier Detection	CNN	95.10	0.93	0.96
Lu et al. (2025) – CNN + Channel Coherence	CNN	93.50	0.85	0.90
Ponnada et al. (2024) – TinyML + NASNet-XGBoost	Hybrid	97.20	0.96	0.98
Ma et al. (2023) – CNN-BiLSTM	Deep Learning	97.80	0.97	0.98
Hu et al. (2023) – Hybrid Transformer	Transformer	98.10	0.98	0.99
Gao et al. (2023) – Prototypical Part Network	Deep Learning	97.60	0.96	0.98
Hosseinzadeh et al. (2024) – Ensemble BiLSTM	Ensemble	98.52	0.963	0.993
Lu et al. (2023) – CBAM 3D CNN-BiLSTM	Attention	97.95	0.98	0.99
Representative Hybrid Quantum Learning (Biomedical)	Quantum	96–99	0.95–0.99	0.98–1.00
Proposed EfficientNet-B0 + QCNN	Hybrid Quantum–Classical	99.50	0.99	1.000

Note: Performance values reported in the literature are obtained using different datasets, preprocessing strategies, and evaluation protocols. Therefore, the comparison is intended to provide a general performance reference rather than a direct benchmark.

In addition to outperforming recent classical approaches, the proposed framework demonstrated competitive performance relative to representative hybrid quantum learning models reported for biomedical classification. Unlike many existing quantum studies that rely on generic variational circuits or focus on image classification tasks, the proposed method integrates temporal–spectral EEG representations with a lightweight four-qubit QCNN optimized for hybrid end-to-end learning. Complementary analyses of cross-validation, trainability, expressibility, feature separability, and computational scalability further indicate that the observed performance is achieved with a stable optimization behavior rather than solely through an increased model complexity.

IX. Ablation Study

To quantify the contributions of the individual components of the proposed hybrid quantum–classical framework, four complementary analyses were conducted. These investigations examine the impact of the classical feature extraction pipeline, variational quantum representation learning module, selected quantum architecture, and computational cost associated with the hybrid model. Together, these analyses provide insights into the effectiveness, efficiency, and practical feasibility of the proposed framework for EEG seizure classification.

A. Component-Wise Architectural Ablation

To evaluate the contribution of each major component, progressively enhanced model configurations were constructed by incrementally incorporating CWT-based preprocessing, EfficientNet-B0 feature extraction, variational quantum representation learning, and the proposed quantum attention mechanism (QAM). The experimental results are presented in Table VI.

TABLE VI. COMPONENT-WISE ARCHITECTURAL ABLATION

Configuration	CWT	EfficientNet-B0	QCNN	Attention	Test Accuracy (%)
Raw EEG + SVM	✗	✗	✗	✗	76.3
CWT + SVM	✓	✗	✗	✗	81.5
CWT + EfficientNet-B0 + FC	✓	✓	✗	✗	96.0
CWT + EfficientNet-B0 + QCNN	✓	✓	✓	✗	98.5
Proposed Framework	✓	✓	✓	✓	**99.5**

The results demonstrate a consistent improvement in the classification performance as additional components are incorporated into the framework. Transforming EEG signals into CWT scalograms improved the performance over the conventional SVM baseline by providing richer temporal–spectral representations. Incorporating EfficientNet-B0 yielded the largest performance gain, increasing the classification accuracy by 14.5 percentage points relative to the CWT-SVM configuration. Replacing the classical fully connected classifier with the variational QCNN further improved the accuracy by 2.5 pp, indicating that quantum-enhanced representation learning provides complementary discriminative information beyond classical latent features. Finally, the proposed patch-level quantum attention mechanism produced an additional 1.0 percentage point improvement while enhancing the qualitative interpretability of seizure-sensitive regions.

B. Variational Quantum Circuit Design Analysis

The proposed framework employs a customized shallow four-qubit variational quantum circuit designed to balance expressive representation learning, optimization stability, and computational efficiency under the constraints of noisy intermediate-scale quantum (NISQ) computing. The circuit combines trainable rotational gates with ring-topology entanglement to capture nonlinear interactions among compressed EEG feature representations while maintaining a shallow circuit depth that is suitable for efficient simulation. The effectiveness of the proposed circuit is supported by multiple complementary analyses presented in this study, including expressibility evaluation, barren plateau analysis, trainability assessment, feature-space separability analysis, and overall classification performance. Collectively, these results indicate that the selected circuit architecture maintains a stable optimization behavior while learning discriminative quantum-enhanced latent representations for seizure classification. Although comparisons with alternative variational circuit architectures (e.g., RealAmplitudes, Hardware-Efficient Ansatz, and StronglyEntanglingLayers) were beyond the scope of this study, the proposed circuit demonstrated consistent optimization stability and competitive predictive performance within the adopted hybrid learning framework. A systematic comparison of different variational circuit designs under identical experimental settings will be conducted in future studies.

C. Qubit Count Analysis

The influence of the quantum circuit size was investigated by varying the number of qubits while maintaining the remaining network configuration unchanged. The results are presented in Table VII.

TABLE VII. QUBIT COUNT ANALYSIS

Qubits	Accuracy (%)	Circuit Depth	Training Runtime (s)	Trainable Parameters	Assessment
1	91.0	5	~180	~50,177	Underfitting
2	94.5	7	~450	~50,450	Below Optimal
3	97.0	9	~890	~50,723	Good
4	**99.5**	**11**	**2815**	**56,094**	**Selected**
5	99.0	13	~4200	~57,367	Higher Cost

Increasing the number of qubits progressively improved the classification performance by enabling richer quantum feature representations. However, larger quantum circuits also increase the circuit depth, simulation time, and computational complexity. Although the five-qubit configuration achieved a comparable predictive performance, the additional computational overhead did not provide a meaningful improvement over the four-qubit model. These results indicate that increasing the circuit size does not necessarily improve the classification performance and may reduce the computational efficiency. Consequently, the four-qubit configuration provides the most suitable balance between the predictive accuracy, optimization stability, and computational cost for the proposed framework.

D. Computational Cost Versus Predictive Performance

To assess whether the additional computational cost introduced by the quantum component is justified, the predictive performance of the hybrid framework was compared with that of its classical counterpart. The comparison is summarized in Table VIII.

TABLE VIII. PERFORMANCE–COMPLEXITY TRADE-OFF

Model	Test Accuracy (%)	Trainable Parameters	Relative Computational Cost
EfficientNet-B0 + FC	96.0	~54k	Lower
EfficientNet-B0 + QCNN	98.5	~56k	Moderate
Proposed Framework	99.5	56,094	Moderate

The hybrid quantum–classical framework introduces only a modest increase in model complexity while providing measurable improvements in predictive performance. Compared with the classical EfficientNet-B0 classifier, the incorporation of the variational QCNN improved the classification accuracy by 2.5 pp, whereas the addition of the quantum attention mechanism further enhanced the accuracy and interpretability. Although quantum circuit simulation increases the computational overhead relative to a purely classical implementation, the observed improvement in seizure classification performance supports the practical effectiveness of the proposed hybrid architecture under the evaluated experimental conditions.

X. Discussion

The proposed hybrid quantum–classical framework demonstrated strong performance on the UCI Epileptic Seizure Recognition Dataset, achieving a five-fold cross-validation accuracy of 97.80% ± 1.50% and a held-out test accuracy of 99.50%, indicating a stable predictive performance under the adopted evaluation protocol. The relatively low variation across the cross-validation folds suggests that the framework generalizes consistently within the balanced benchmark dataset. The component-wise ablation study showed that the hybrid QCNN module improved the classification performance compared with the corresponding classical EfficientNet-B0 baseline, suggesting that quantum-enhanced representation learning provides complementary discriminative information for seizure classification. However, because this study did not experimentally compare the proposed variational circuit with alternative quantum ansatz architectures or equivalently parameterized classical models, the observed improvement should be interpreted as evidence of the effectiveness of the proposed hybrid framework rather than definitive proof of the superiority of the quantum representation itself. Additional analyses, including expressibility evaluation, barren plateau analysis, trainability assessment, feature-space visualization, robustness analysis, and computational scalability, collectively provide supporting evidence that the proposed shallow variational circuit remains trainable and computationally feasible under simulation-based NISQ conditions. Furthermore, the patch-level quantum attention maps qualitatively highlight seizure-sensitive temporal–spectral regions within the EEG scalograms, improving the interpretability of learned representations. However, these attention maps represent model responses and do not constitute clinically validated biomarkers. Future studies involving expert neurological annotation and quantitative localization metrics are required to establish their clinical significance. Although the proposed framework was evaluated using classical quantum simulation, the results indicate that hybrid quantum–classical learning is a promising research direction in biomedical EEG analysis. Additional validation on larger multicenter datasets, subject-independent evaluation protocols, and real quantum hardware is necessary to fully assess the practical clinical applicability of the proposed approach.

XI. Limitations and Future Work

Despite these encouraging results, several limitations should be acknowledged. First, an experimental evaluation was conducted on a balanced subset of 4,000 EEG segments derived from the publicly available UCI Epileptic Seizure Recognition Dataset. Although the stratified five-fold cross-validation demonstrated stable performance, additional validation on larger, more heterogeneous, multicenter clinical datasets and subject-independent evaluation protocols is necessary to further establish the generalizability of the proposed framework. Second, all quantum experiments were performed using classical simulations rather than execution on physical quantum processors. Consequently, practical hardware limitations, including gate errors, decoherence, measurement shot noise, limited qubit connectivity, and readout errors, were not incorporated into the experimental evaluation. These factors may reduce the classification performance and increase inference variability when deploying the framework on current noisy intermediate-scale quantum (NISQ) hardware. Third, the proposed study investigates a customized shallow variational quantum circuit but does not experimentally compare alternative variational circuit architectures, such as hardware-efficient ansatz, real amplitudes, or strongly entangling layers, under identical experimental conditions. Similarly, comparisons with equivalently parameterized classical architectures remain an important direction for future research. Finally, although patch-level quantum attention maps improve qualitative interpretability, their correspondence with clinically meaningful seizure regions has not yet been validated quantitatively.

Future work will therefore focus on the following: evaluation on larger multicenter EEG datasets, subject-independent seizure classification, implementation on real quantum hardware with quantum error mitigation, comparative studies involving alternative quantum ansatz designs and comparable classical architectures, quantitative validation of attention localization using expert neurological annotation.

XII. Conclusion

This study presents a hybrid quantum–classical framework for EEG-based epileptic seizure classification by integrating Continuous Wavelet Transform (CWT)-based temporal–spectral representations, EfficientNet-B0 feature extraction, and a shallow four-qubit variational Quantum Convolutional Neural Network (QCNN). Experimental evaluation on a balanced subset of the UCI Epileptic Seizure Recognition Dataset achieved a mean five-fold cross-validation accuracy of 97.80 ± 1.50% and a held-out test accuracy of 99.50%, demonstrating consistent performance under the adopted evaluation protocol. Comprehensive analyses, including ablation studies, optimization stability, expressibility, barren plateau behavior, robustness evaluation, computational scalability, and quantum attention visualization, indicate that the proposed hybrid framework learns discriminative quantum-enhanced representations while remaining trainable within the constraints of simulation-based NISQ environments. The component-wise ablation study further showed measurable performance improvements over the corresponding classical baseline, suggesting that the hybrid quantum component provides complementary representational capability for classifying seizures. The current implementation is limited to simulation-based quantum execution and benchmark dataset evaluation; therefore, the findings should be interpreted as an investigation of the potential of hybrid quantum–classical learning, rather than evidence of immediate clinical deployment. As quantum hardware continues to mature, future validation on larger clinical datasets and real quantum devices will be essential to further assess the practical utility of hybrid quantum machine learning in intelligent EEG analysis.

DECLARATIONS

Competing Interests: The authors declare no competing interests.

Funding Information: This research received no specific funding from public, commercial, or not-for-profit agencies.

Author Contributions: A.S. Athigiri Arulalan: Conceptualization, methodology, software development, data curation, formal analysis, investigation, validation, visualization, writing—original draft, and writing—review and editing. Dr. G. Senthilkumar: Supervision, project administration, and funding acquisition. Dr. L. Jabasheela: Supervision, research oversight, and funding acquisition. Dr. K. Sangeetha: Investigation and funding acquisition. Dr. V. Subedha: Investigation and funding acquisition. Dr. V. Sathiya: Investigation and funding acquisition.

Data Availability Statement: The UCI Epileptic Seizure Recognition Dataset is publicly available. The implementation details required to reproduce the experiments are available from the corresponding author upon reasonable request.

Research Involving Humans and/or Animals: This study used publicly available anonymized EEG data and did not involve direct experimentation on humans or animals.

REFERENCES

[1] Abtahi, A., Ryvlin, P., & Aminifar, A. (2025). Identification of relevant ECG features for epileptic seizure prediction using interpretable machine learning. *IEEE Access* , *13* . https://doi.org/10.1109/ACCESS.2025.3583461

[2] Gao, Y., Liu, A., Wang, L., Qian, R., & Chen, X. (2023). A Self-Interpretable Deep Learning Model for Seizure Prediction Using a Multiscale Prototypical Part Network. *IEEE Transactions on Neural Systems and Rehabilitation Engineering* , *31* , 1847. https://doi.org/10.1109/tnsre.2023.3260845

[3] Grubov, V., Nazarikov, S., Kurkin, S., Utyashev, N., Andrikov, D. A., Карпов, О. Э., & Hramov, A. E. (2024). Two-Stage Approach Combining Outlier Detection Method and Deep Learning Enhances Automatic Epileptic Seizure Detection. *IEEE Access* , *12* , 122168. https://doi.org/10.1109/access.2024.3453039

[4] Guo, L., Yu, T., Zhao, S., Li, X., Liao, X., & Li, Y. (2023). CLEP: Contrastive Learning for Epileptic Seizure Prediction Using a Spatiotemporal-Spectral Network. *IEEE Transactions on Neural Systems and Rehabilitation Engineering* , *31* , 3915. https://doi.org/10.1109/tnsre.2023.3322275

[5] Hosseinzadeh, M., Khoshvaght, P., Sadeghi, S., Asghari, P., Varzeghani, A. N., Mohammadi, M., Mohammadi, H., Lánský, J., & Lee, S.-W. (2024). A Model for Epileptic Seizure Diagnosis Using the Combination of Ensemble Learning and Deep Learning. *IEEE Access* , *12* , 137132. https://doi.org/10.1109/access.2024.3457018

[6] Hu, S., Liu, J., Yang, R., Wang, Y., Wang, A., Li, K., Liu, W., & Yang, C. (2023). Exploring the Applicability of Transfer Learning and Feature Engineering in Epilepsy Prediction Using Hybrid Transformer Model. *IEEE Transactions on Neural Systems and Rehabilitation Engineering* , *31* , 1321. https://doi.org/10.1109/tnsre.2023.3244045

[7] Jana, R., & Mukherjee, I. (2023). Efficient Seizure Prediction and EEG Channel Selection Based on Multi-Objective Optimization. *IEEE Access* , *11* , 54112. https://doi.org/10.1109/access.2023.3281450

[8] Kapoor, B., & Nagpal, B. (2024). Gradient boosting for predicting relations between biomedical signals and seizures using LightGBM and XGBoost. *J Mob Multimed* , *20* , 359. https://doi.org/10.13052/JMM1550-4646.2024

[9] Li, C., Deng, Z., Song, R., Liu, X., Qian, R., & Chen, X. (2022). EEG-Based Seizure Prediction via Model Uncertainty Learning. *IEEE Transactions on Neural Systems and Rehabilitation Engineering* , *31* , 180. https://doi.org/10.1109/tnsre.2022.3217929

[10] Lian, Q., Wang, Y., & Qi, Y. (2025). Dynamic Instance-Level Graph Learning Network of Intracranial Electroencephalography Signals for Epileptic Seizure Prediction. *IEEE Journal of Biomedical and Health Informatics* , *29* (11), 8348. https://doi.org/10.1109/jbhi.2025.3578627

[11] Liu, S., Wang, J., Li, S., & Cai, L. (2023). Epileptic Seizure Detection and Prediction in EEGs Using Power Spectra Density Parameterization. *IEEE Transactions on Neural Systems and Rehabilitation Engineering* , *31* , 3884. https://doi.org/10.1109/tnsre.2023.3317093

[12] Lu, S., Liu, L., Li, J., Chambers, J. D., Cook, M., & Grayden, D. B. (2025). Leveraging Channel Coherence in Long-Term iEEG Data for Seizure Prediction. *IEEE Journal of Biomedical and Health Informatics* , *29* (8), 5541. https://doi.org/10.1109/jbhi.2025.3556775

[13] Lu, X., Wen, A., Sun, L., Wang, H., Guo, Y., & Ren, Y. (2023). An Epileptic Seizure Prediction Method Based on CBAM-3D CNN-LSTM Model. *IEEE Journal of Translational Engineering in Health and Medicine* , *11* , 417. https://doi.org/10.1109/jtehm.2023.3290036

[14] Ma, Y., Huang, Z., Su, J., Shi, H., Wang, D., Jia, S., & Li, W. (2023). A Multichannel Feature Fusion CNN-Bi-LSTM Epilepsy EEG Classification and Prediction Model Based on Attention Mechanism. *IEEE Access* , *11* , 62855. https://doi.org/10.1109/access.2023.3287927

[15] Oliveira, A., Pinto, M. F., Lopes, F., Leal, A., & Teixeira, C. (2024). Classifier Combination Supported by the Sleep-Wake Cycle Improves EEG Seizure Prediction Performance. *IEEE Transactions on Biomedical Engineering* , *71* (8), 2341. https://doi.org/10.1109/tbme.2024.3368304

[16] Ponnada, S., Tan, K. T., Kshirsagar, P. R., Rao, P. S., & Dayal, A. (2024). Expanding Applications of TinyML in Versatile Assistive Devices: From Navigation Assistance to Health Monitoring System Using Optimized NASNet-XGBoost Transfer Learning. *IEEE Access* , *12* , 168328. https://doi.org/10.1109/access.2024.3496791

[17] Premavathi, T., Shukla, M., & Jadeja, R. (2024a). Predicting patient-specific epileptic seizures from scalp EEG using KNN with transfer learning. *IEEE Access* , *12* . https://doi.org/10.1109/ACCESS.2024.3521457

[18] Qi, N., Piao, Y., Wang, Q., Li, X., & Wang, Y. (2024). Semi-Supervised Seizure Prediction Based on Deep Pairwise Representation Alignment of Epileptic EEG Signals. *IEEE Access* , *12* , 119056. https://doi.org/10.1109/access.2024.3447901

[19] Shi, S., & Liu, W. (2023). B2-ViT Net: Broad Vision Transformer Network With Broad Attention for Seizure Prediction. *IEEE Transactions on Neural Systems and Rehabilitation Engineering* , *32* , 178. https://doi.org/10.1109/tnsre.2023.3346955

[20] Sook, J., Li, T., & Li, Y. (2024). Epileptic Seizure Prediction Based on Synchroextracting Transform and Sparse Representation. *IEEE Access* , *12* , 187684. https://doi.org/10.1109/access.2024.3514859

[21] Varnosfaderani, S. M., McNulty, I., Sarhan, N. J., Abood, W., & Alhawari, M. (2024). An Efficient Epilepsy Prediction Model on European Dataset With Model Evaluation Considering Seizure Types. *IEEE Journal of Biomedical and Health Informatics* , *28* (10), 5842. https://doi.org/10.1109/jbhi.2024.3423766

[22] Wang, X., Zhang, C., Kärkkäinen, T., Chang, Z., & Cong, F. (2022). Channel Increment Strategy-Based 1D Convolutional Neural Networks for Seizure Prediction Using Intracranial EEG. *IEEE Transactions on Neural Systems and Rehabilitation Engineering* , *31* , 316. https://doi.org/10.1109/tnsre.2022.3222095

[23] Wang, Y., Cui, W., Yu, T., Li, X., Liao, X., & Li, Y. (2023). Dynamic Multigraph Convolution-Based Channel-Weighted Transformer Feature Fusion Network for Epileptic Seizure Prediction. *IEEE Transactions on Neural Systems and Rehabilitation Engineering* , *31* , 4266. https://doi.org/10.1109/tnsre.2023.3321414

[24] Wang, Y., Shi, Y., Cheng, Y., He, Z., Wei, X., Chen, Z., & Zhou, Y. (2022). A Spatiotemporal Graph Attention Network Based on Synchronization for Epileptic Seizure Prediction. *IEEE Journal of Biomedical and Health Informatics* , *27* (2), 900. https://doi.org/10.1109/jbhi.2022.3221211

[25] Wei, B., Xu, L., & Zhang, J. (2024). A Compact Graph Convolutional Network With Adaptive Functional Connectivity for Seizure Prediction.

IEEE Transactions on Neural Systems and Rehabilitation Engineering , *32* , 3531. https://doi.org/10.1109/tnsre.2024.3460348

[26] Wu, D., Shi, Y., Wang, Z., Yang, J., & Sawan, M. (2023). C2SP-Net: Joint Compression and Classification Network for Epilepsy Seizure Prediction. *IEEE Transactions on Neural Systems and Rehabilitation Engineering* , *31* , 841. https://doi.org/10.1109/tnsre.2023.3235390